# Evaluation of Two-Stage Soft-Switched Flyback Micro-inverter for Photovoltaic Applications

Sinan Zengin and Mutlu Boztepe

Ege University, Electrical and Electronics Engineering Department, Izmir, Turkey
sinan.zengin@ege.edu.tr, mutlu.boztepe@ege.edu.tr

## Abstract

**The research on the micro inverters for photovoltaic (PV) applications has been increased in recent years due to its advantages of minimization of module mismatch losses, the elimination of serial diode losses, and suitability for mass production etc. However, the micro-inverters suffer from the low voltage at the input PV terminals that causes high conduction loss and requires large electrolytic capacitors for decoupling purposes. The electrolytic capacitors have relatively low lifetime in comparison with the PV modules, and restricts the micro-inverter service life significantly. Moreover, the high conduction loss decreases the micro-inverters conversion efficiency considerably. In order to mitigate these drawbacks, two stage micro-inverters are generally proposed. In this study, a 200 W two stage soft switched flyback micro-inverter is designed for highest efficiency, and compared with the conventional single stage flyback micro-inverter. By using two-stage soft-switched flyback micro-inverter, the decoupling capacitor value is decreased by 10 times, and maximum efficiency is increased by 13.7%. The experimental results are also presented.**

## 1. Introduction

The installed solar PV capacity is growing faster than other renewable technologies during the period from end-2006 through 2011 with increasing an average of %58 annually [1]. PV power installation trend is large-scale ground-mounted system, but rooftop small scale systems play also an important role. PV systems can be classified into two categories; stand-alone and grid connected. Due to intermittent characteristic of solar irradiation, large scale batteries are required in stand-alone PV systems. On the other hand, the grid connected PV systems use the utility grid as an infinite storage element, and hence, eliminate the batteries which have high cost and low life time [2].

Grid-tied PV systems are connected to the utility grid through an inverter. Central and string type inverters operate at a single common operating point for all PV modules attached to the inverter, and hence mismatching or partially shading of PV modules create considerable MPP losses. In micro-inverter technology, each PV module has their own DC-AC inverter, and therefore can be operated at its own maximum power point (MPPT) [3].

Micro-inverters can be designed as single stage or two stages for single phase utility connection [4], where the maximum instantaneous power injected to the grid is twice of the PV module average power. Therefore, a power decoupling circuit is necessary in order to obtain instantaneous power balance. Capacitors as an energy reservoir are used simply for power decoupling purposes [5]. However, decoupling capacitor value at low voltage level may become very large when total harmonic distortion (THD) and PV utilization ratio are taken into account [6]. Electrolytic capacitors are usually used in the decoupling circuits due to advantages of low cost and high capacitance. Unfortunately, it has very low life time when compared to the PV modules (>20 years), and therefore not suitable for using in micro-inverter circuits when considering lifetime.

Although single stage micro-inverters have simple structure and easy control, it suffers from the low input PV voltage. The power decoupling circuits working at low voltage requires usually electrolytic capacitors. Additionally the conduction losses increase at low voltage/high current conditions. As an alternative, in two stage micro-inverters, the PV voltage is boosted at the first stage and the power decoupling function is realized at high voltage side which reduces the decoupling capacitor value considerably. Thus the film capacitors can be used and the micro-inverter life time is lengthened. On the other hand, having two power conversion stages may reduce the overall conversion efficiency significantly, but soft switching techniques can mitigate this problem [7]. Despite its several advantageous, two stage topologies have complicated structure, high cost and difficult to control.

In the literature, micro-inverters are well reviewed [8–10] and the flyback based topology is the most attractive one because of simple current control, low part counts and potentially low cost. Flyback type micro-inverters have three operating modes; such as discontinuous (DCM), continuous (CCM) and boundary conduction modes (BCM) [10-11]. Since the injected current into the grid can be modulated by open loop control without current sensor, the DCM operation is usually preferred.

In order to amplify the PV voltage in the first stage, many candidate soft switched converters were proposed in the literature [13–16]. These are mainly classified as isolated, non-isolated DC/DC PWM converters and resonant converters. Since the second stage isolates the PV module from the grid, non-isolated converters can be used for efficiency consideration. Furthermore, the isolated DC/DC PWM converters can be preferred where high voltage gain is required. On the other hand, resonant converters may not operate efficiently under wide load range such as PV power whose power ranges from zero to rated power during the day.

In this study, a two-stage soft-switched flyback micro-inverter is designed and compared with a conventional counterpart. In the first and second stages, a single-switch soft-switched boost DC/DC converter and DCM soft-switched flyback inverter are implemented respectively [16-17]. This paper is organized as follows; the analysis of conventional DCM flyback micro-inverter and two-stage soft-switched flyback micro-inverter are given in the sections 2 and 3, respectively. The experimental results are presented in the section 4.

## 2. Conventional DCM Flyback Micro-inverter

Conventional DCM flyback micro-inverter topology is given in Fig. 1. The main switch S1 is turned on for the duration of $t_{on}$, and a certain amount of energy is stored in magnetizing inductance $L_m$. The stored energy is transferred to the secondary side by turning off the S1 during $t_{off}$ time through the switches S2-D1 or S3-D2 (depending on the grid voltage positive or negative cycle). For DCM operation, the total time ($t_{on}$+$t_{off}$) must be shorter than switching frequency period $T_s$. By using this property, the maximum duty ratio $d_p$ (=$t_{on}/T_s$ ) can be expressed as [10];

$$d_p = \frac{1}{1+(V_{dc}/nV_{gm})} \tag{1}$$

where $V_{dc}$ is the input PV MPPT voltage, $V_{gm}$ is the maximum grid voltage and $n$ is the transformer turn ratio.

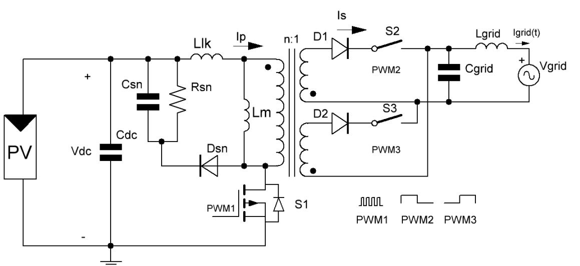


**Fig. 1.** Conventional DCM Flyback Topology

Despite the main switch $S_1$ turns on softly with zero current, it has considerable switching loss at turn-off. On the other hand, the drain voltage of the mosfet is clamped by the RCD snubber circuit ($R_{sn}$-$C_{sn}$-$D_{sn}$) [12], and therefore the leakage inductance energy which can be assumed as 2.5% of the energy stored in $L_m$ [18], is dissipated in the snubber resistor $R_{sn}$. Moreover the conduction loss on the main switch is high, since the rms value of $I_p$ is relatively large due to low input dc voltage. The rms input current can be written as follows [10], [18];

$$I_{p,rms} = \sqrt{\frac{64}{9\pi}\frac{P^2}{d_p V_{dc}^2}} \tag{2}$$

where $P$ is the maximum PV power. It should be noted that, $I_{p,rms}$ depends inversely on the $V_{dc}$. Hence, if the input DC voltage increases, $I_{p,rms}$ decreases and the conduction loss in the primary circuit reduces significantly.

On the other hand, the decoupling capacitor value can be calculated by [5];

$$C_{dc} = \frac{P}{2\pi V_{dc} f_{grd} \Delta V_{dc}} \tag{3}$$

where $f_{grd}$ is the grid frequency and $\Delta V_{dc}$ is peak-to-peak DC bus ripple voltage. Instantaneous input power and the DC bus voltage are depicted in Fig. 2.

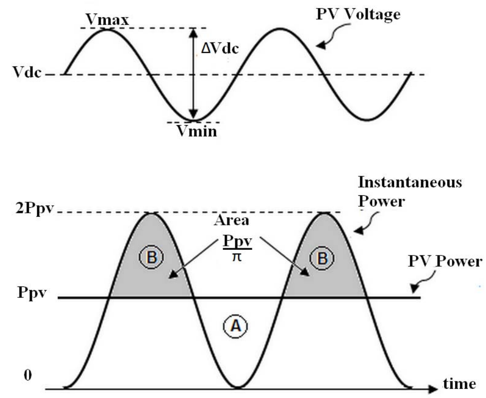


**Fig. 2.** DC bus voltage and instantaneous input power

The switching frequency harmonics on the output current $I_{grid}$ are filtered by the output filter $C_{grid}$-$L_{grid}$. However, the low frequency harmonics that are created by the DC-bus voltage ripple are not filtered by the output filter [6]. In order to keep these harmonics at low level, we proposed the voltage ripple $\Delta V_{dc}$ as 5% by taking into consideration the THD and PV utilization ratio [6]. Consequently, all parameters used in the analysis of conventional DCM flyback circuit are listed in Table 1.

**Table 1.** Conventional DCM Flyback Micro-inverter Parameter Values

| ***Parameter*** | ***Value*** | | ***Parameter*** | ***Value*** |
|---|---|---|---|---|
| $n$ | 0.1428 | | $C_{grid}$ | 0.33 uF |
| $d_p$ | 0.55 | | $R_{sn}$ | 1.67 kΩ |
| $L_m$ | 6.64 uH | | $C_{sn}$ | 100 nF |
| $L_{lk}$ | 0.2 uH | | $C_{dc}$ | 6 mF |
| $L_{grid}$ | 1.75 mH | | $f_{s,f}$ | 75 Khz |

## 3. Two-Stage Soft-Switched Flyback Micro-inverter

The block diagram of a two-stage flyback micro-inverter is shown in Fig. 3. In this topology, both the MPPT and PV voltage amplification tasks are achieved in the first stage and DC/AC inversion is realized in the second stage. In this study, the intermediate DC-bus voltage is selected as 110 V, and also soft switching techniques are employed in both stages.

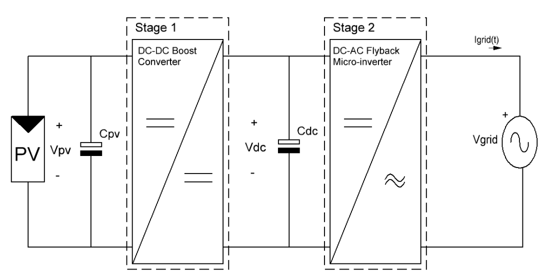


**Fig. 3.** The Block Diagram of Two-stage Flyback Micro-inverter

### 3.1. The Soft-switched DC/DC Boost Converter

The DC/DC boost converter shown in Fig. 4 is selected for the first stage because of the features such that single switch, easy to control, high efficiency and soft switching [16]. This converter has two coupled inductors and a resonance capacitor to implement the soft switching.

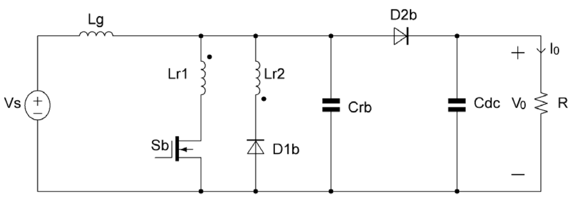


**Fig. 4.** Soft-Single-Switched Boost Converter

The soft switching operation of the converter is briefly as follows: Before turn on the switch $S_b$, the current in the inductors $L_{r1}$ and $L_{r2}$ are zero, the diode $D_{2b}$ current is equal to output current $I_0$ , and $C_{rb}$ capacitor voltage is equal to the output voltage $V_0$ in steady state. When the switch $S_b$ is turned on, the switch current increases linearly due to series inductor $L_{r1}$ and soft turn on occurs at zero current. When the switch current reaches to $I_0$, the current in diode $D_{2b}$ becomes zero and it is turned off at zero current. From this moment, $C_{rb}$ and $L_{r1}$ start to resonance and $L_{r1}$ gets all the energy of $C_{rb}$, and then the voltage of capacitor $C_{rb}$ reduces to zero. Later, the diode $D_{1b}$ turns on under zero voltage and small circulating current flows through coupled inductors during the switch $S_b$ on-time. Due to zero voltage at capacitor $C_{rb}$, the switch $S_b$ is turned off at zero voltage, and the current in $L_{r1}$ inductor is transferred to $L_{r2}$, and the capacitor $C_{rb}$ starts to charge. In order to guarantee the soft switching operation, the minimum values for resonant elements $L_{r1}$ and $C_{rb}$ can be expressed as [16];

$$C_{rb} > C_{rb,\min} = \frac{I_{sw} t_{k,s}}{2V_{sw}} \qquad (4)$$
$$L_{r1} > L_{r1,\min} = \frac{V_{sw} t_{a,s}}{I_{sw}}$$

where $I_{sw}$ is the current of switch $S_b$ before turn off, $t_{k,s}$ is the switch current fall time, $V_{sw}$ is the voltage of switch $S_b$ after turn off, and $t_{a,s}$ is the switch current rise time.

The filter element $L_g$ can be designed as in the case of conventional boost converter. Since the $C_{dc}$ is the DC-bus capacitor of second stage, it acts as decoupling capacitor, and therefore should be sized according to (3). The parameters of the designed circuit are listed in Table 2.

**Table 2.** Parameters of the Boost Converter

| ***Parameter*** | ***Value*** | | ***Parameter*** | ***Value*** |
|---|---|---|---|---|
| $L_{r1}$ | 15 uH | | $L_g$ | 130 uH |
| $L_{r2}$ | 112 uH | | $C_{dc}$ | 600 uF |
| $C_{rb}$ | 10 nF | | $f_{s,b}$ | 100 kHz |

### 3.2. The Soft-switched DCM Flyback Micro-inverter

The soft-switched DCM flyback topology employed in the second stage of the micro-inverter is given in Fig. 5 [17]. In this topology, an auxiliary circuit composed of $D_{a1}$, $D_{a2}$, $L_r$, $C_r$ and $S_a$ is added to conventional DCM flyback micro-inverter in order to obtain soft switching and active-clamp operations. The energy stored in the leakage inductance is transferred back to the DC bus and the overall efficiency is improved.

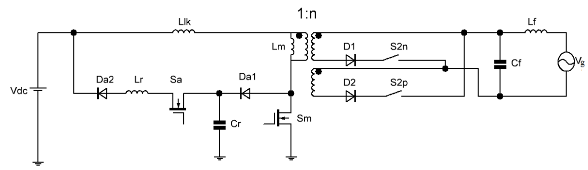


**Fig. 5.** Soft Switched DCM Flyback Micro-inverter

The soft switching operation of the converter is briefly as follows: $S_m$ and $S_a$ switches turn on and off together. Before turn on the switches, the inductors $L_m$ and $L_r$ have zero current; therefore soft turn-on is obtained at zero current for both switches. The switch $S_m$ turns off softly at zero voltage due to parallel capacitor $C_r$. Since the current through the switch $S_a$ is zero at this moment, the switch $S_a$ is also turned off at zero current [19]. All diodes and switches are soft-switched in this topology, and the leakage inductance energy is recycled. Hence, high switching frequency can be chosen, and thus, efficiency improvement can be obtained. $L_m$, $n$, $L_f$ and $C_f$ are selected as in the conventional flyback inverter [10]. The resonant elements $L_r$ and $C_r$ values should be selected by using (4) as mentioned before. The parameters of the designed circuit are listed in Table 3.

**Table 3.** Parameters of the Soft-switched DCM Flyback Micro-inverter

| ***Parameter*** | ***Value*** | | ***Parameter*** | ***Value*** |
|---|---|---|---|---|
| $n$ | 3 | | $C_r$ | 10 nF |
| $d_p$ | 0,5 | | $L_f$ | 1,75 mH |
| $L_m$ | 57 uH | | $C_f$ | 0,33 uF |
| $L_{lk}$ | 0,75 uH | | $C_{dc}$ | 600 uF |
| $L_r$ | 24 uH | | $f_{s,f}$ | 75 Khz |

## 4. Experimental Results

The prototypes of single-stage conventional DCM flyback micro-inverter and two-stage soft-switched DCM flyback micro-inverter were realized as shown in Fig. 6 (a) and (b) respectively The input power to micro-inverter was taken from the laboratory DC power supply (GW Instek Spd-3606).

DC bus voltage of the two stage micro-inverter and the output voltage of micro-inverter are shown in Fig. 8 while 377Ω resistor is used as a load. It can be seen from the figure that, the frequency of DC bus voltage variation is twice of the frequency of the output voltage, and the average DC bus voltage is equal to 110V as expected.

The soft switching operations are verified for the two-stage micro-inverter as shown in the figures 9-12. The boost converter's main switch ($S_b$) turn on and turn off waveforms can be seen in Fig. 9 and Fig. 10 respectively. Turn on occurs at zero current and turn off occurs at zero voltage. The soft switched flyback inverter's main switch ($S_m$) turn on and turn off waveforms can be seen in Fig. 11. Similarly, the switch turns on at zero current and turn off at zero voltage. Turn on and off characteristics of auxiliary switch ($S_a$) are given in Fig.12 where the switch turns on and off at zero current.

The efficiency curve with respect to the input power for both topologies were measured and are shown Fig. 7. At 145 W input power, while the efficiency for the conventional DCM flyback micro-inverter is 78%, it is 88.7% for the two-stage soft-switched DCM flyback micro-inverter. The European efficiency [18] is improved from 83.3% to 86.8% as expected.

For 7% DC bus voltage ripple ($=\Delta V_{dc}/V_{dc}$*100%), required capacitor capacity is calculated and used as 6000 uF and 600 uF for conventional and two-stage soft-switched flyback micro-inverter respectively. When 377 Ω resistor is used as load, THD of the injected current is 3.5% for the both inverters as expected from [6].

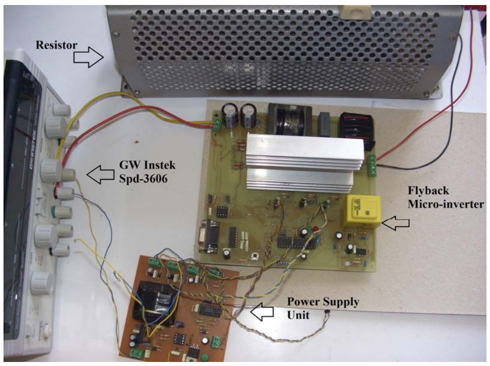


(a)

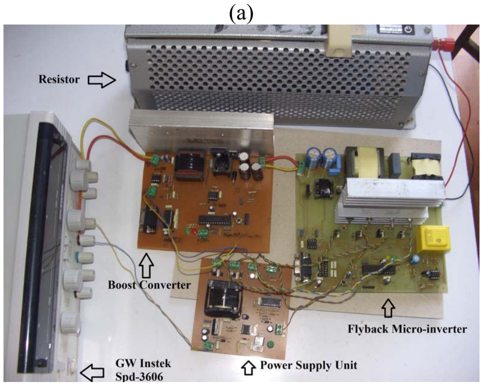


(b)

**Fig. 6.** (a) Conventional Flyback Micro-inverter (b) Two-stage Soft-Switched Flyback Micro-inverter

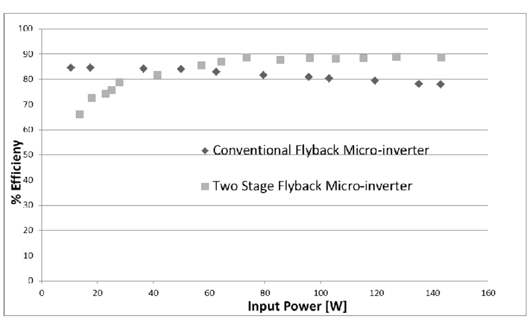


**Fig. 7.** Efficiency Measurement of Conventional and Two-stage Soft -switched DCM Flyback Micro-inverters

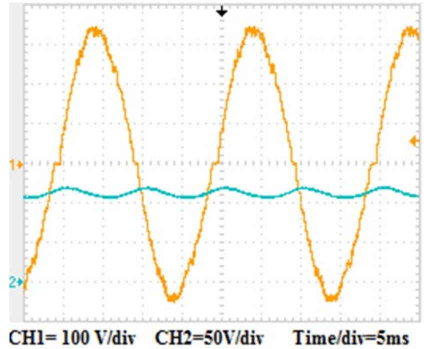


**Fig. 8.** DC Bus Voltage Variation and Output Voltage through 377 Ω resistor

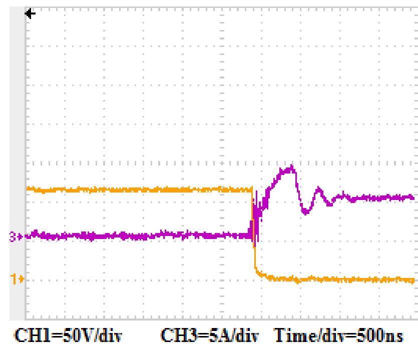


**Fig. 9.** The $S_b$ switch's turn on time

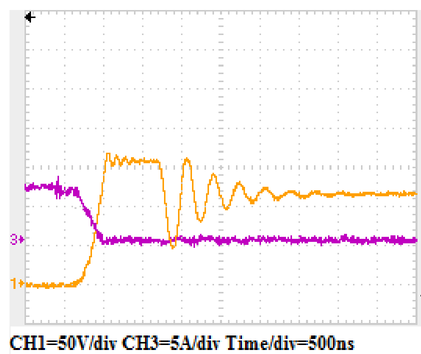


**Fig. 10.** The $S_b$ switch's turn off time

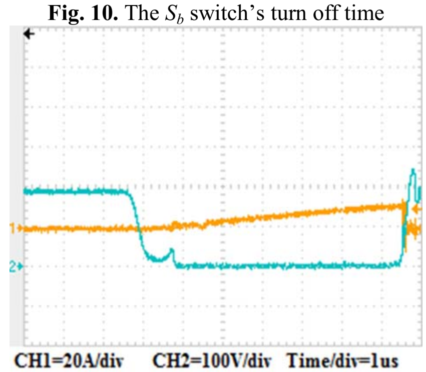


**Fig. 11.** The $S_m$ switch's turn on and turn off times

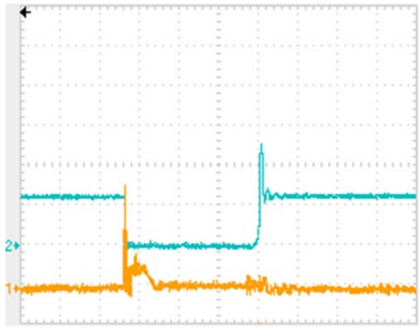


**Fig. 12.** The $S_a$ switch's turn on and turn off times

## 5. Conclusion

Single-stage conventional DCM flyback micro-inverter and two-stage soft-switched DCM flyback micro-inverter were analyzed and experimentally compared. By boosting the input DC voltage, decoupling capacitor value reduced from 6000 uF to 600 uF, and efficiency is increased from 78% to 88.7%. Moreover, decreasing the decoupling capacitor value can lead to change electrolytic capacitors with film types which extends the inverter life time further. However, two-stage soft switched flyback micro-inverter brings extra switching elements and passive components. As a result of this, cost and control complexity increase.

## 7. References


[1] "Renewables 2012 Global Status Report",2012, Available: http://www.map.ren21.net/GSR/GSR2012_low.pdf.

[2] D. P. Kaundinya, P. Balachandra, and N. H. Ravindranath, "Grid-connected versus stand-alone energy systems for decentralized power—A review of literature," Renewable and Sustainable Energy Reviews, vol. 13, no. 8, pp. 2041–2050, Oct. 2009.

[3] S. V. Dhople, J. L. Ehlmann, A. Davoudi, and P. L. Chapman, "Multiple-input boost converter to minimize power losses due to partial shading in photovoltaic modules," in 2010 IEEE Energy Conversion Congress and Exposition, 2010, no. c, pp. 2633–2636.

[4] S. B. Kjaer, J. K. Pedersen, and F. Blaabjerg, "A Review of Single-Phase Grid-Connected Inverters for Photovoltaic Modules," IEEE Trans. on Industry Applications, vol. 41, no. 5, pp. 1292–1306, 2005.

[5] H. Hu, S. Harb, N. Kutkut, I. Batarseh, and Z. J. Shen, "A Review of Power Decoupling Techniques for Microinverters With Three Different Decoupling Capacitor Locations in PV Systems," IEEE Tran. on Power Electronics, vol. 28, no. 6, pp. 2711–2726, 2013.

[6] S. Zengin, F. Deveci, and M. Boztepe, "Decoupling Capacitor Selection in DCM Flyback PV Microinverters Considering Harmonic Distortion," IEEE Transactions on Power Electronics, vol. 28, no. 2, pp. 816–825, Feb. 2013.

[7] G. H. Tan, J. Z. Wang, and Y. C. Ji, "Soft-switching flyback inverter with enhanced power decoupling for photovoltaic applications," IET Electric Power Applications, vol. 1, no. 2, pp. 264–274, 2007.

[8] Y. Xue, L. Chang, and S. B. Kjær, "Topologies of Single-Phase Inverters for Small Distributed Power Generators: An Overview," IEEE Tran. on Power Electronics, vol. 19, no. 5, pp. 1305–1314, 2004.

[9] Q. Li and P. Wolfs, "A Review of the Single Phase Photovoltaic Module Integrated Converter Topologies With Three Different DC Link Configurations," IEEE Tran. on Power Electronics, vol. 23, no. 3, pp. 1320–1333, 2008.

[10] A. C. Kyritsis, E. C. Tatakis, and N. P. Papanikolaou, "Optimum Design of the Current-Source Flyback Inverter for Decentralized Grid-Connected Photovoltaic Systems," IEEE Tran. on Energy Conversion, vol. 23, no. 1, pp. 281–293, 2008.

[11] Y. Li and R. Oruganti, "A Low Cost Flyback CCM Inverter for AC Module Application," IEEE Transactions on Power Electronics, vol. 27, no. 3, pp. 1295–1303, Mar. 2012.

[12] F. Semiconductor, "Application Note AN-4147 Design Guidelines for RCD Snubber of Flyback Converters." 2006.

[13] A. Emrani, E. Adib, and H. Farzanehfard, "Single-Switch Soft-Switched Isolated DC-DC Converter," IEEE Tran. on Power Electronics, vol. 27, no. 4, pp. 1952–1957, 2012.

[14] S. Park, G. Cha, Y. Jung, and C. Won, "Design and Application for PV Generation System Using a Soft-Switching Boost Converter With SARC," IEEE Trans. on Industrial Electronics, vol. 57, no. 2, pp. 515–522, 2010.

[15] H.-W. Seong, H.-S. Kim, K. Park, G.-W. Moon, and M.-J. Youn, "High Step-Up DC-DC Converters Using Zero-Voltage Switching Boost Integration Technique and Light-Load Frequency Modulation Control," IEEE Tran. on Power Electronics, vol. 27, no. 3, pp. 1383–1400, 2012.

[16] M. R. Amini and H. Farzanehfard, "Novel Family of PWM Soft-Single-Switched DC-DC Converters With Coupled Inductors," IEEE Trans. on Industrial Electronics, vol. 56, no. 6, pp. 2108–2114, 2009.

[17] J. Elmes, C. Jourdan, O. A. Rahman, and I. Batarseh, "High-Voltage, High-Power- Density DC-DC Converter for Capacitor Charging Applications," in Applied Power Electronics Conference and Exposition, 2009, pp. 433–439.

[18] A. C. Nanakos, E. C. Tatakis, N. P. Papanikolaou, and S. Member, "A Weighted-Efficiency-Oriented Design Methodology of Flyback Inverter for AC Photovoltaic Modules," IEEE Tran. on Power Electronics, vol. 27, no. 7, pp. 3221–3233, 2012.

[19] S. Zengin, "Two Stage Soft Switched Flyback Type Photovoltaic Micro-inverter Design", M.S. Thesis, Graduate School of Natural and Applied Sciences, Ege University , Izmir, Turkey, 2013.